Progress In Electromagnetics Research, Vol. 119, 85–105, 2011

TAYLOR-ORTHOGONAL BASIS FUNCTIONS FOR THE DISCRETIZATION IN METHOD OF MOMENTS OF SECOND KIND INTEGRAL EQUATIONS IN THE SCATTERING ANALYSIS OF PERFECTLY CONDUCTING OR DIELECTRIC OBJECTS

E. Ubeda, J. M. Tamayo, and J. M. Rius*

AntennaLab, Department of Signal Theory and Communications (TSC), Universitat Politècnica de Catalunya (UPC), Campus Nord UPC, D-3, C/Jordi Girona, 1-3, Barcelona 08034, Spain

Abstract—We present new implementations in Method of Moments of two types of second kind integral equations: (i) the recently proposed Electric-Magnetic Field Integral Equation (EMFIE), for perfectly conducting objects, and (ii) the Müller formulation, for homogeneous or piecewise homogeneous dielectric objects. We adopt the Taylor-orthogonal basis functions, a recently presented set of facet-oriented basis functions, which, as we show in this paper, arise from the Taylor's expansion of the current at the centroid of the discretization triangles. We show that the Taylor-orthogonal discretization of the EMFIE mitigates the discrepancy in the computed Radar Cross Section observed in conventional divergence-conforming implementations for moderately small, perfectly conducting, sharp-edged objects. Furthermore, we show that the Taylor-discretization of the Müller-formulation represents a valid option for the analysis of sharp-edged homogenous dielectrics, especially with low dielectric contrasts, when compared with other RWG-discretized implementations for dielectrics. Since the divergence-Taylor Orthogonal basis functions are facet-oriented, they appear better suited than other, edge-oriented, discretization schemes for the analysis of piecewise homogenous objects since they simplify notably the discretization at the junctions arising from the intersection of several dielectric regions.

Received 17 May 2011, Accepted 22 June 2011, Scheduled 21 July 2011

* Corresponding author: Juan Manuel Rius (rius@tsc.upc.edu).

1. INTRODUCTION

The discretization in Method of Moments (MoM) with RWG basis functions, a zeroth-order example of divergence-conforming set, of the Magnetic-Field Integral Equation (MFIE) [1, 2], a second kind surface integral equation, for perfectly conducting (PeC) objects shows some discrepancy [3] in the computed Radar Cross Section (RCS) with respect to the EFIE [4], a first kind surface integral equation [5]. This discrepancy is especially evident in the analysis of electrically moderately small perfectly conducting sharp-edged objects. Over the last years, other sets of basis functions have been proposed for the MoM-discretization of the MFIE in the scattering analysis of PeC-objects that reduce the observed discrepancy [6–10].

The Müller formulation [11–13] stands for a second kind Integral Equation in the scattering analysis of homogeneous or piecewise homogeneous dielectric objects. The MoM-implementation of the Müller-formulation is normally carried out with the RWG basis functions [13, 14]. Since the Müller formulation combines magnetic-field and electric-field contributions from the PeC-case in such a way that the gram-matrix contributions are enhanced, one may expect that this implementation of the Müller-formulation may reproduce, to some extent, the observed performance for the RWG-discretization of the MFIE in conductors. In our experience, as we show in this paper, the Poggio-Miller-Chang-Harrington-Wu-Tsai (PMCHWT) formulation [15–17], a first kind Integral Equation for dielectric objects, provides a stable trend for convergence for electrically coarser degrees of meshing than the Müller-formulation. Moreover, we observe that moderately small sharp-edged objects with low dielectric contrast show in general much smaller RCS deviation with the RWG-implementation of the Müller-formulation than in the PeC-case. However, for high dielectric contrasts, the observed degree of deviation increases, although it depends greatly on the shape of the object under analysis. In view of our tests, the RCS deviation becomes especially significant for cubes, as it has been also reported by others [13, 14].

In this paper, we use the recently presented facet-oriented orthogonal basis functions [18], well-suited for the discretization of Second-kind Integral Equations. We now decide to rename the first order orthogonal basis functions presented in [18] as divergence-Taylor-Orthogonal basis functions (div-TO) because, as we show in this paper, they are derived from the uniform terms and from the linear, divergence-conforming, contributions in the 2D Taylor's expansion of the current at a reference surface point inside a facet arising from the discretization. We present two new MoM-

implementations with the div-TO basis functions of two second kind Integral Equations: (i) The Electric-Magnetic Field Integral Equation (EMFIE), recently presented in [19] under a Loop-Star discretization [20, 21], for conductors and (ii) the Müller formulation, for homogeneous or piecewise homogeneous dielectric objects. The development of the div-TO discretization of the EMFIE and the Müller formulation, unlike the same implementation for the MFIE in [18], requires the discretization of the scalar potentials. The source contributions of the scalar potentials are usually discretized in the context of the EFIE or PMCHWT formulations with divergence-conforming basis functions [4, 22], which preserve normal continuity of the current across the edges. In this paper, though, we provide a more general definition for the discrete electric and magnetic scalar potentials because the normal component of the current expanded with the div-TO basis functions is not confined in the facets arising from the discretization.

2. TAYLOR-ORTHOGONAL BASIS FUNCTIONS

Interestingly, the imposition of the tangential continuity of the current across edges appears better-suited than the imposition of the normal continuity for the MoM-discretization of the MFIE for sharp-edged objects [6]. The normal-continuity constraint in RWG is applied in the discretizations of the EFIE but it is not clear, in our opinion, that it must be imposed for second kind Integral Equations like the MFIE or the EMFIE.

The current may become singular exactly on the tips of sharp edges [23] but is bounded and continuous at any surface point $\vec{r}_0$ out of sharp edges or corners. In general, we can approximate the current in the vicinity of the reference point $\vec{r}_0$, $\mathbf{J}(\vec{r}_0|u,v)$, in terms of the first-order 2D Taylor's expansion, as

$$\begin{aligned}\mathbf{J}(\vec{r}_0|u,v) &\approx \mathbf{J}_{(0,0)} + \left[\frac{\partial \mathbf{J}}{\partial u}\right]_{(0,0)} u + \left[\frac{\partial \mathbf{J}}{\partial v}\right]_{(0,0)} v \\ &= [J_u]_{(0,0)}\hat{u} + [J_v]_{(0,0)}\hat{v} + \left[\frac{\partial J_u}{\partial u}\right]_{(0,0)} u\hat{u} \\ &+ \left[\frac{\partial J_v}{\partial u}\right]_{(0,0)} u\hat{v} + \left[\frac{\partial J_u}{\partial v}\right]_{(0,0)} v\hat{u} + \left[\frac{\partial J_v}{\partial v}\right]_{(0,0)} v\hat{v} \quad (1)\end{aligned}$$

where (u,v) stand for the local cartesian planar coordinates around $\vec{r}_0$, and $\mathbf{J}_{(0,0)}$, $[\frac{\partial \mathbf{J}}{\partial u}]_{(0,0)}$, $[\frac{\partial \mathbf{J}}{\partial v}]_{(0,0)}$ denote the current and the partial derivatives of the current at $\vec{r}_0$. The definition of the following

quantities A, B, C, D

$$A = \left[\frac{\partial J_u}{\partial u}\right]_{(0,0)} + \left[\frac{\partial J_v}{\partial v}\right]_{(0,0)} \qquad B = \left[\frac{\partial J_u}{\partial u}\right]_{(0,0)} - \left[\frac{\partial J_v}{\partial v}\right]_{(0,0)} \tag{2}$$

$$C = \left[\frac{\partial J_v}{\partial u}\right]_{(0,0)} + \left[\frac{\partial J_u}{\partial v}\right]_{(0,0)} \qquad D = \left[\frac{\partial J_v}{\partial u}\right]_{(0,0)} - \left[\frac{\partial J_u}{\partial v}\right]_{(0,0)} \tag{3}$$

allows the expression of (1) equivalently as

$$\begin{aligned}\mathbf{J}\left(\vec{r}_0|u,v\right) \approx\ & [J_u]_{(0,0)}\hat{u} + [J_v]_{(0,0)}\hat{v} + \frac{1}{2}(A+B)u\hat{u} \\ & + \frac{1}{2}(C+D)u\hat{v} + \frac{1}{2}(C-D)v\hat{u} + \frac{1}{2}(A-B)v\hat{v}\end{aligned} \tag{4}$$

and

$$\begin{aligned}\mathbf{J}\left(\vec{r}_0|u,v\right) \approx\ & [J_u]_{(0,0)}\hat{u} + [J_v]_{(0,0)}\hat{v} + \frac{A}{2}(u\hat{u} + v\hat{v}) \\ & + \frac{B}{2}(u\hat{u} - v\hat{v}) + \frac{C}{2}(u\hat{v} + v\hat{u}) + \frac{D}{2}(u\hat{v} - v\hat{u})\end{aligned} \tag{5}$$

where the local polar coordinates (ρ, ϕ) and the local cartesian coordinates (u, v) are related as (see Figure 1)

$$\rho\hat{\rho} = u\hat{u} + v\hat{v} \qquad \rho\hat{\phi} = u\hat{v} - v\hat{u} \tag{6}$$

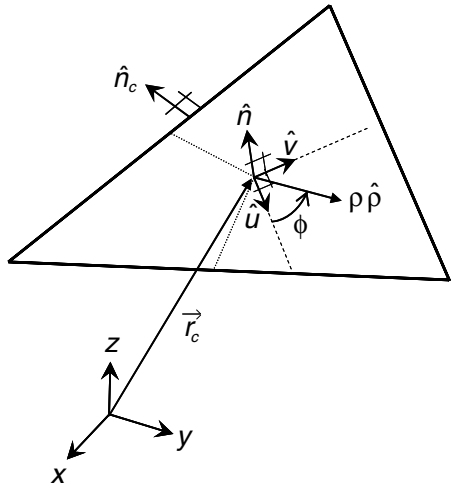

Figure 1. Local polar and cartesian coordinates for the definition of the Taylor-Orthogonal basis functions.

In view of (2) and (3), the definitions for A and D become

$$A = [\nabla \cdot \mathbf{J}]_{(0,0)} \qquad D = [\hat{n} \cdot \nabla \times \mathbf{J}]_{(0,0)} \tag{7}$$

The coefficients A, D are important in the linear approximation of $\mathbf{J}$ at $\vec{r}_0$ because $[\nabla \cdot \mathbf{J}]_{(0,0)}$ and $[\hat{n} \cdot \nabla \times \mathbf{J}]_{(0,0)}$ are relevant in the expansion of the normal components of the Electric and Magnetic scattered fields, respectively. However, the remaining terms in (5), associated to the coefficients C, B, provide null divergence and normal curl, whereby they may be ignored. The expression (5) can be then rewritten accordingly as

$$\mathbf{J}\left(\vec{r}_0|u,v\right) \approx [J_u]_{(0,0)}\hat{u} + [J_v]_{(0,0)}\hat{v} + \frac{1}{2}[\nabla\cdot\mathbf{J}]_{(0,0)}\rho\hat{\rho} + \frac{1}{2}[\hat{n}\cdot\nabla\times\mathbf{J}]_{(0,0)}\rho\hat{\phi} \tag{8}$$

which represents a local linear approximation of the current in the vicinity of the reference point $\vec{r}_0$ with four degrees of freedom: $[J_u]_{(0,0)}$, $[J_v]_{(0,0)}$, $[\nabla \cdot \mathbf{J}]_{(0,0)}$ and $[\hat{n} \cdot \nabla \times \mathbf{J}]_{(0,0)}$. Four basis functions are hence required to capture each of the unknowns. We establish as domains for these basis functions each of the facets arising from the discretization.

The zeroth order Taylor-orthogonal basis functions [25] are

$$\mathbf{b}_{0,u} = \frac{1}{\sqrt{A_r}}\hat{u} \qquad \mathbf{b}_{0,v} = \frac{1}{\sqrt{A_r}}\hat{v} \tag{9}$$

where A_r represents the area of the facet. This definition allows

$$\int_F \mathbf{b}_{0,u} \cdot \mathbf{b}_{0,v} ds = 0 \tag{10}$$

$$\int_F \mathbf{b}_{0,u} \cdot \mathbf{b}_{0,u} ds = \int_F \mathbf{b}_{0,v} \cdot \mathbf{b}_{0,v} ds = 1 \tag{11}$$

where F denotes the facet. We define the remaining first-order basis functions as

$$\mathbf{b}_{1,\rho} = \frac{1}{2A_r}\left(\vec{r} - \vec{r}_c\right) \qquad \mathbf{b}_{1,n\times\rho} = \frac{1}{2A_r}\hat{n} \times \left(\vec{r} - \vec{r}_c\right) \tag{12}$$

where $\vec{r}_c$ stands for the geometrical center of the facet, the centroid in a triangle (see Figure 1). From this definition it is accomplished

$$\nabla \cdot \mathbf{b}_{1,\rho} = \hat{n} \cdot (\nabla \times \mathbf{b}_{1,n\times\rho}) = 1/A_r \tag{13}$$

$$\int_F \mathbf{b}_{0,u} \cdot \mathbf{b}_{1,\rho} ds = \int_F \mathbf{b}_{0,v} \cdot \mathbf{b}_{1,\rho} ds = \int_F \mathbf{b}_{1,\rho} \cdot \mathbf{b}_{1,n\times\rho} ds = 0 \tag{14}$$

The properties (10) and (14) show that these basis functions are orthogonal, whereby we name them Taylor-orthogonal basis

functions. We define two sets of Taylor-orthogonal basis functions: the divergence-Taylor-orthogonal basis functions (div-TO) and the curl-Taylor-orthogonal basis functions (curl-TO). Both sets of basis functions group three Taylor-orthogonal basis functions per facet. Whereas the div-TO set retains $\mathbf{b}_{0,u}$, $\mathbf{b}_{0,v}$ and $\mathbf{b}_{1,\rho}$, the curl-TO set considers $\mathbf{b}_{0,u}$, $\mathbf{b}_{0,v}$ and $\mathbf{b}_{1,n\times\rho}$.

The monopolar RWG and nxRWG sets [10, 24] stand for facet-oriented sets of basis functions too. They arise from breaking, respectively, the normal or tangential continuity constraints enforced by the RWG or nxRWG sets across the edges. The div-TO and the curl-TO sets expand the same spaces of current as, respectively, the monopolar RWG and the monopolar nxRWG sets [18]. Therefore, the monopolar sets and the div-TO or curl-TO basis functions require the same number of unknowns. Indeed, twice the number of edges is equal, for closed objects, to three times the number of facets. This represents twice the number of unknowns of the RWG basis functions.

3. TAYLOR-ORTHOGONAL DISCRETIZATION OF THE ELECTRIC-MAGNETIC FIELD INTEGRAL EQUATION

The Electric-Magnetic Field Integral Equation (EMFIE) is based on imposing at the same time the tangential magnetic and the normal electric field boundary conditions over the surface S embracing the scatterer; that is,

$$\hat{n} \times \mathbf{H}^i = \frac{\mathbf{J}}{\mathbf{2}} - \left(\frac{1}{\mu_0}\right) \hat{n} \times [\nabla \times \mathbf{A}]_{\mathrm{CPV}} \tag{15}$$

$$\frac{\hat{n} \cdot \mathbf{E}^i}{\eta_0} = \frac{\nabla \cdot \mathbf{J}}{2(-jk)} + \left(\frac{1}{\eta_0}\right) \hat{n} \cdot [\nabla \Phi]_{\mathrm{CPV}} + \left(\frac{jk}{\mu_0}\right) \hat{n} \cdot \mathbf{A} \tag{16}$$

which are second-kind integral equations because the source magnitudes, current and divergence of the current, respectively, $\mathbf{J}$ and $\nabla \cdot \mathbf{J}$, come out from the source-integrals in the potentials. $\mathbf{H}^i$, $\mathbf{E}^i$ stand for the incident magnetic and electric fields and the quantities k, $\hat{n}$, ε_0, μ_0, η_0 represent, respectively, the wavenumber, the unit vector normal to the surface, the free-space dielectric permittivity, the free-space magnetic permeability and the free-space impedance. The MFIE is obtained by imposing only the tangential continuity of the magnetic field in (15).

The limiting values of the singular Kernel contributions in the source integrals depend on the current for the magnetic field in (15) and on the divergence of the current for the normal component of the scattered electric field in (16). The definition for the magnetic vector

potential $\mathbf{A}$ is

$$\mathbf{A} = \mu_0 \iint\limits_S G\mathbf{J}ds' \tag{17}$$

The definition of the potential related quantities in (15) and (16) capturing the Cauchy Principal value of the surface integrals are

$$[\nabla \times \mathbf{A}]_{\text{CPV}} = \mu_0 \iint\limits_{S,\text{CPV}} \nabla G \times \mathbf{J}ds' \tag{18}$$

$$[\nabla \Phi]_{\text{CPV}} = \frac{\eta_0}{(-jk)} \iint\limits_{S,\text{CPV}} \nabla G \nabla' \cdot \mathbf{J}ds' \tag{19}$$

where $G = \frac{e^{-jk|\vec{r}-\vec{r}'|}}{4\pi|\vec{r}-\vec{r}'|}$ stands for the free-space Green's function.

In view of (15) and (16), the source magnitudes appear predominantly in the range spaces of the integral equations derived. It makes then sense to undertake the MoM-testing of (15) with the basis functions adopted for the expansion of the current. Similarly, in the MoM-testing of (16) we need to employ the divergence of the basis functions expanding the current. It is then clear that a successful MoM-implementation of the EMFIE must provide for the proper expansion for both the current and the charge density. The solenoidal contribution of the current has zero divergence and cannot therefore expand properly the range space of the normal-electric integral equation in (16). The nonsolenoidal component of the current, with non-null divergence, is well suited for the expansion of the charge density, which is mandatory for the proper accomplishment of (16). Therefore, the MoM-implementation of the EMFIE with the Loop, solenoidal, and the Star, nonsolenoidal, basis functions follows these guidelines accordingly [19].

The RWG discretization of the MFIE provides some deviation in the computed RCS of sharp-edged perfectly conducting objects with respect to the EFIE. The EMFIE, based to some extent on the MFIE, also shows this RCS discrepancy with the Loop-Star discretization, which represents a solenoidal-nonsolenoidal rearrangement of the RWG current space. In the div-TO discretization, the solenoidal subspace of current must be captured by the divergence-free zeroth-order terms, $\mathbf{b}_{0,u}$, $\mathbf{b}_{0,v}$. The $\mathbf{b}_{1,\rho}$ term, in contrast, with non-zero divergence, must provide for the expansion of the nonsolenoidal subspace of current. Furthermore, the monopolar RWG discretization of the MFIE reduces significantly the RCS deviation observed with the RWG discretization for moderately small sharp-edged objects [10]. Since the div-TO basis functions expand the same space as the monopolar RWG set, it is

reasonable to expect some improvement in the div-TO discretization of the EMFIE too with respect to the Loop-Star discretization.

We arrange the divergence-Taylor-Orthogonal basis functions in three subsets $\mathbf{B}_{0,u} = \{\mathbf{b}_{0,u}^1 \ \ldots \ \mathbf{b}_{0,u}^{N_f}\}$, $\mathbf{B}_{0,v} = \{\mathbf{b}_{0,v}^1 \ \ldots \ \mathbf{b}_{0,v}^{N_f}\}$ and $\mathbf{B}_{1,\rho} = \{\mathbf{b}_{1,\rho}^1 \ \ldots \ \mathbf{b}_{1,\rho}^{N_f}\}$ gathering, respectively, the u-, v- and ρ-contributions in the N_f facets arising from the discretization. These subsets are introduced consecutively in the definition of $\{\mathbf{o}_n\}$, the whole set of divergence-Taylor-Orthogonal basis functions, so that $\{\mathbf{o}_n\} = \{\mathbf{B}_{0,u}, \mathbf{B}_{0,v}, \mathbf{B}_{1,\rho}\}$. The expansion of the electric current with the div-TO basis functions then yields

$$\mathbf{J} \approx \sum_{n=1}^{3N_f} J_n \mathbf{o}_n \tag{20}$$

where J_n denote the current coefficients. The div-TO discretization of the EMFIE results in the following matrix system

$$H_m^i = \sum_{n=1}^{3N_f} Z_{mn}^H J_n \qquad m = 1 \ \ldots \ 2N_f \tag{21}$$

$$E_m^i = \sum_{n=1}^{3N_f} Z_{mn}^E J_n \qquad m = (2N_f + 1) \ \ldots \ 3N_f \tag{22}$$

The magnetic-field quantities Z_{mn}^H and H_m^i denote, respectively, the impedance matrix elements and the tested incident magnetic field or excitation vector, defined as

$$H_m^i = \left[\left\langle \mathbf{o}_m, \hat{n}_m \times \mathbf{H}^i \right\rangle\right] = \iint_{F_m} (\mathbf{o}_m \times \hat{n}_m) \cdot \mathbf{H}^i ds \tag{23}$$

$$Z_{mn}^H = \frac{1}{2} \iint_{F_m} \mathbf{o}_m \cdot \mathbf{o}_n ds - \frac{1}{\mu_0} \iint_{F_m} \mathbf{o}_m \cdot (\hat{n}_m \times [\nabla \times \mathbf{A}]_{\mathrm{CPV}}^n) \, ds \tag{24}$$

where F_m stands for the m-th facet arising from the discretization and $\hat{n}_m$ denotes the unit vector normal normal to F_m.

The first term in the right-hand side in (24) is related with the Gram-matrix, which is diagonal because of the property of orthogonality of the div-TO basis functions. The testing in (23) and (24) is carried out with the zeroth-order Taylor-orthogonal basis functions [25]. In view of (18), the contribution of the n-th div-TO basis function in the expansion of $[\nabla \times \mathbf{A}]_{\mathrm{CPV}}$ becomes

$$[\nabla \times \mathbf{A}]_{\mathrm{CPV}}^n = \mu_0 \iint_{F_n, \mathrm{CPV}} \nabla G \times \mathbf{o}_n ds' \tag{25}$$

The electric-field quantities Z^E_{mn} and E^i_m in (22) denote, respectively, the normal-electric impedance elements and the normally tested incident electric field, which are defined as

$$E^i_m = \left[\left\langle \Pi_m \hat{n}_m, \frac{\mathbf{E}^i}{\eta_0} \right\rangle\right] = \left(\frac{1}{\eta_0}\right) \iint\limits_{F_m} \Pi_m \hat{n}_m \cdot \mathbf{E}^i ds \tag{26}$$

$$\begin{aligned} Z^E_{mn} &= \frac{1}{2(-jk)} \iint\limits_{F_m} \Pi_m \nabla \cdot \mathbf{o}_n ds + \frac{1}{\eta_0} \iint\limits_{F_m} \Pi_m \hat{n}_m \cdot [\nabla \Phi]^n_{\mathrm{CPV}} ds \\ &\quad + \left(\frac{jk}{\mu_0}\right) \iint\limits_{F_m} \Pi_m \hat{n}_m \cdot \mathbf{A}^n ds \end{aligned} \tag{27}$$

where Π_m stands for a constant pulse defined over the testing facet. The definition of this testing-pulse is consistent with the uniformity of the divergence of the term $\mathbf{b}_{1,\rho}$ in the div-TO set. In view of (17), the n-th div-TO contribution in the discrete expansion of the magnetic vector potential in (27) results in

$$\mathbf{A}^n = \mu_0 \iint\limits_{F_n} \mathbf{o}_n G ds' \tag{28}$$

Furthermore, $[\nabla \Phi]^n_{\mathrm{CPV}}$, the other potential magnitude in (27), denotes the contribution of the n-th div-TO basis function to the Cauchy Principal value of the gradient of the electric scalar potential.

The use of the potentials in the analysis of PeC-scattering problems with Integral Equations is associated with the accomplishment of the Gauge-Lorentz condition, which, prior to discretization, establishes the definition of the electric scalar potential Φ in terms of the magnetic vector potential $\mathbf{A}$ as

$$\Phi = -\frac{1}{jk\sqrt{\mu_0 \varepsilon_0}} \nabla \cdot \mathbf{A} = -\frac{\eta_0}{jk} \nabla \cdot \left[\iint\limits_S G \mathbf{J} ds' \right] \tag{29}$$

After discretization, the space of current is determined by the expansion in terms of the adopted divergence-Taylor-Orthogonal basis n-th div-TO basis function in the expansion of the electric scalar potential is

$$\Phi^n = -\frac{\eta_0}{jk} \nabla \cdot \left[\iint\limits_{F_n} G \mathbf{o}_n ds' \right] \tag{30}$$

which becomes equivalently

$$\begin{aligned}\Phi^n &= -\frac{\eta_0}{jk}\iint_{F_n}\nabla G\cdot\mathbf{o}_n ds = \frac{\eta_0}{jk}\iint_{F_n}\nabla' G\cdot\mathbf{o}_n ds' \\ &= \frac{\eta_0}{jk}\left[\iint_{F_n}\nabla'\cdot(G\mathbf{o}_n)ds' - \iint_{F_n} G\nabla'\cdot(\mathbf{o}_n)ds'\right] \\ &= \frac{\eta_0}{jk}\left[\oint_{\partial F_n} G\,(\mathbf{o}_n\cdot\hat{n}_c)\,dl' - \iint_{F_n} G\nabla'\cdot(\mathbf{o}_n)ds'\right] \qquad (31)\end{aligned}$$

where ∂F_n and $\hat{n}_c$ denote, respectively, the closed contour around the source facet F_n and the unit-normal vector to this contour (see Figure 1). Note that the line-integral in (31) becomes zero for divergence-conforming discretizations, like RWG or rooftop, because they ensure, by definition, normal continuity of the current across the edges. As a matter of fact, this leads to the widely used expression for $[\nabla\Phi]^n_{\mathrm{CPV}}$ arising for example in divergence-conforming discretizations of the EFIE [4, 22]. However, the current expanded by the divergence-Taylor-Orthogonal basis functions leaks out from the facet domain and therefore the full expression in (31) needs to be considered. Finally, the expression for $[\nabla\Phi]^n_{\mathrm{CPV}}$ required in (27) must be

$$[\nabla\Phi]^n_{\mathrm{CPV}} = \frac{1}{j\omega\varepsilon_0}\left[\oint_{\partial F_n}\nabla G\,(\mathbf{o}_n\cdot\hat{n}_c)\,dl' - \iint_{F_n,\mathrm{CPV}}\nabla G\nabla'\cdot(\mathbf{o}_n)ds'\right] \qquad (32)$$

4. TAYLOR-ORTHOGONAL DISCRETIZATION OF THE MÜLLER FORMULATION

The Müller formulation arises in the scattering analysis of homogeneous or piecewise homogeneous dielectric objects. In general, the EM scattering from a penetrable object is solved through the definition of an equivalent problem resulting from the combination of two homogeneous problems associated to the outer and inner dielectric regions, respectively R_1 and R_2, in general with different pairs of dielectric permittivities and magnetic permeabilities, (ε_1, μ_1) and (ε_2, μ_2). Both regions have accordingly different wavenumbers and impedances, (k_1, η_1) and (k_2, η_2). In particular, the Müller formulation results from imposing the following magnetic-field and electric-field conditions across

the surface S embracing the penetrable object so that

$$\mu_1\hat{n}_1 \times \mathbf{H}^i = \frac{(\mu_1+\mu_2)}{2}\mathbf{J}_1 - \mu_1\hat{n}_1 \times [\mathbf{H}_1^s]_{\text{CPV}} + \mu_2\hat{n}_2 \times [\mathbf{H}_2^s]_{\text{CPV}} \quad (33)$$

$$\varepsilon_1\hat{n}_1 \times \mathbf{E}^i = -\frac{(\varepsilon_1+\varepsilon_2)}{2}\mathbf{M}_1 - \varepsilon_1\hat{n}_1 \times [\mathbf{E}_1^s]_{\text{CPV}} + \varepsilon_2\hat{n}_2 \times [\mathbf{E}_2^s]_{\text{CPV}} \quad (34)$$

which are second-kind integral equations because the source magnitudes, the electric and magnetic currents, come out from the source radiating integrals of the scattered fields. The terms $\mathbf{E}^i$, $\mathbf{H}^i$ denote the incident electric and magnetic fields. The vectors $\hat{n}_1$, $\hat{n}_2$ denote the unit vectors normal to the surface pointing into the outer and inner regions, respectively, and accomplish $\hat{n}_2 = -\hat{n}_1$. The electric and magnetic currents at both sides of the surface, $\mathbf{J}_1$, $\mathbf{J}_2$ and $\mathbf{M}_1$, $\mathbf{M}_2$, are also related so that $\mathbf{J}_2 = -\mathbf{J}_1$ and $\mathbf{M}_2 = -\mathbf{M}_1$. The scattered magnetic and electric fields at the outer and inner sides of the surface stand for $\mathbf{H}_1^s$, $\mathbf{H}_2^s$ and $\mathbf{E}_1^s$, $\mathbf{E}_2^s$. The extraction of the limiting value of the singular Kernel contribution in the source integrals of the scattered fields results in

$$\hat{n}_i \times \mathbf{H}_i^s = \frac{\mathbf{J}_i}{2} + \hat{n}_i \times [\mathbf{H}_i^s]_{\text{CPV}} \quad (35)$$

$$\hat{n}_i \times \mathbf{E}_i^s = -\frac{\mathbf{M}_i}{2} + \hat{n}_i \times [\mathbf{E}_i^s]_{\text{CPV}} \quad (36)$$

where $i = 1, 2$ denotes the dielectric region involved.

The contributions to the scattered fields in (33) and (34) in terms of the vector and scalar potentials in each region become

$$\mu_i\hat{n}_i \times \mathbf{H}_i^s = \frac{\mu_i\mathbf{J}_i}{2} + \hat{n}_i \times [\nabla \times \mathbf{A}_i]_{\text{CPV}} - jk_i\eta_i\hat{n}_i \times \mathbf{F}_i - \mu_i\hat{n}_i \times \nabla\Psi_i \quad (37)$$

$$\varepsilon_i\hat{n}_i \times \mathbf{E}_i^s = -\frac{\varepsilon_i\mathbf{M}_i}{2} - \hat{n}_i \times [\nabla \times \mathbf{F}_i]_{\text{CPV}} - \frac{jk_i}{\eta_i}\hat{n}_i \times \mathbf{A}_i - \varepsilon_i\hat{n}_i \times \nabla\Phi_i \quad (38)$$

The integral expressions for the magnetic vector and the electric scalar potentials, $\mathbf{A}_i$ and Φ_i, related with the electric source currents, yield

$$\mathbf{A}_i = \mu_i \iint\limits_S G_i\mathbf{J}_i ds' \qquad \Phi_i = \frac{\eta_i}{(-jk_i)} \iint\limits_S G_i\nabla' \cdot \mathbf{J}_i ds' \quad (39)$$

Similarly, the integral expressions for the electric vector and magnetic scalar potentials, related with the magnetic source currents, become

$$\mathbf{F}_i = \varepsilon_i \iint\limits_S G_i\mathbf{M}_i ds' \qquad \Psi_i = \frac{1}{(-jk_i\eta_i)} \iint\limits_S G_i\nabla' \cdot \mathbf{M}_i ds' \quad (40)$$

where $G_i = \frac{e^{-jk_i|\vec{r}-\vec{r}'|}}{4\pi|\vec{r}-\vec{r}'|}$ stands for the Green's function in the region R_i.

The Galerkin-discretization of the Müller-formulation with the div-TO basis functions is formally similar to the procedure described in [13] for the RWG basis functions. Now the expansion of the electric and magnetic currents with the div-TO basis functions is

$$\mathbf{J}_1 \approx \sum_{n=1}^{3N_f} J_n^1 \mathbf{o}_n \qquad \mathbf{M}_1 \approx \sum_{n=1}^{3N_f} M_n^1 \mathbf{o}_n \tag{41}$$

where J_n^1 and M_n^1 denote the electric and magnetic current coefficients, respectively, in region R_1. The current coefficients at the other side of the surface, in region R_2 are related so that $J_n^2 = -J_n^1$ and $M_n^2 = -M_n^1$. The div-TO discretization of the Müller-formulation results in the following matrix system

$$H_m^i = \sum_{n=1}^{3N_f} Z_{mn}^{HJ} J_n^1 + \sum_{n=1}^{3N_f} Z_{mn}^{HM} M_n^1 \qquad m = 1 \ \ldots \ 3N_f \tag{42}$$

$$E_m^i = \sum_{n=1}^{3N_f} Z_{mn}^{EJ} J_n^1 + \sum_{n=1}^{3N_f} Z_{mn}^{EM} M_n^1 \qquad m = 1 \ \ldots \ 3N_f \tag{43}$$

The quantities H_m^i and E_m^i represent the excitation vectors for, respectively, the incident magnetic and incident electric fields,

$$H_m^i = \left[\left\langle \mathbf{o}_m, \hat{n}_1^m \times \mathbf{H}^i \right\rangle\right] = \iint_{F_m} (\mathbf{o}_m \times \hat{n}_1^m) \cdot \mathbf{H}^i ds \tag{44}$$

$$E_m^i = \left[\left\langle \mathbf{o}_m, \hat{n}_1^m \times \mathbf{E}^i \right\rangle\right] = \iint_{F_m} (\mathbf{o}_m \times \hat{n}_1^m) \cdot \mathbf{E}^i ds \tag{45}$$

where F_m stands for the m-th facet arising from the discretization of the surface and $\hat{n}_1^m$denotes the unit vector normal to F_m pointing towards the region R_1. The impedance elements in the submatrices along the main diagonal of the system in (42) and (43), Z_{mn}^{HJ} and Z_{mn}^{EM}, are defined as

$$\begin{aligned} Z_{mn}^{HJ} = {} & \frac{(\mu_1 + \mu_2)}{2} \iint_{F_m} \mathbf{o}_m \cdot \mathbf{o}_n ds \\ & - \iint_{F_m} \mathbf{o}_m \cdot [\hat{n}_1^m \times ([\nabla \times \mathbf{A}_1]_{\mathrm{CPV}}^n - [\nabla \times \mathbf{A}_2]_{\mathrm{CPV}}^n)] \, ds \end{aligned} \tag{46}$$

$$Z_{mn}^{EM} = -\frac{(\varepsilon_1+\varepsilon_2)}{2}\iint\limits_{F_m}\mathbf{o}_m\cdot\mathbf{o}_n ds + \iint\limits_{F_m}\mathbf{o}_m\cdot[\hat{n}_1^m\times([\nabla\times\mathbf{F}_1]_{\mathrm{CPV}}^n-[\nabla\times\mathbf{F}_2]_{\mathrm{CPV}}^n)]\,ds \quad (47)$$

where the first term in the right-hand side is related with the Gram-matrix, which is diagonal because of the orthogonality of the div-TO basis functions. The contribution of the n-th div-TO basis function in the expansion of the Cauchy principal value of the source integrals in (46) and (47) yields

$$[\nabla\times\mathbf{A}_1]_{\mathrm{CPV}}^n-[\nabla\times\mathbf{A}_2]_{\mathrm{CPV}}^n=\iint\limits_{S,\mathrm{CPV}}(\mu_1\nabla G_1-\mu_2\nabla G_2)\times\mathbf{o}_n ds' \quad (48)$$

$$[\nabla\times\mathbf{F}_1]_{\mathrm{CPV}}^n-[\nabla\times\mathbf{F}_2]_{\mathrm{CPV}}^n=\iint\limits_{S,\mathrm{CPV}}(\varepsilon_1\nabla G_1-\varepsilon_2\nabla G_2)\times\mathbf{o}_n ds' \quad (49)$$

The definition for the off-diagonal submatrices in (42) and (43), Z_{mn}^{HM} and Z_{mn}^{EJ}, is

$$Z_{mn}^{HM} = -\iint\limits_{F_m}\mathbf{o}_m\cdot[\hat{n}_1^m\times(jk_1\eta_1\mathbf{F}_1^n-jk_2\eta_2\mathbf{F}_2^n)]\,ds - \iint\limits_{F_m}\mathbf{o}_m\cdot[\hat{n}_1^m\times(\mu_1\nabla\Psi_1^n-\mu_2\nabla\Psi_2^n)]\,ds \quad (50)$$

$$Z_{mn}^{EJ} = -\iint\limits_{F_m}\mathbf{o}_m\cdot\left[\hat{n}_1^m\times\left(\frac{jk_1}{\eta_1}\mathbf{A}_1^n-\frac{jk_2}{\eta_2}\mathbf{A}_2^n\right)\right]ds - \iint\limits_{F_m}\mathbf{o}_m\cdot[\hat{n}_1^m\times(\varepsilon_1\nabla\Phi_1^n-\varepsilon_2\nabla\Phi_2^n)]\,ds \quad (51)$$

where the contribution of the n-th div-TO basis function in the expansion of the vector electric and magnetic potentials result in

$$(jk_1\eta_1\mathbf{F}_1^n-jk_2\eta_2\mathbf{F}_2^n)=j\omega\iint\limits_S(\mu_1\varepsilon_1G_1-\mu_2\varepsilon_2G_2)\,\mathbf{o}_n ds' \quad (52)$$

$$\left(\frac{jk_1}{\eta_1}\mathbf{A}_1^n-\frac{jk_2}{\eta_2}\mathbf{A}_2^n\right)=j\omega\iint\limits_S(\mu_1\varepsilon_1G_1-\mu_2\varepsilon_2G_2)\,\mathbf{o}_n ds' \quad (53)$$

and, in view of the discrete expansion of the gradient of the scalar electric potential in the perfectly conducting case in (32), in the

dielectric case the discrete contribution in (51) becomes

$$(\varepsilon_1 \nabla\Phi_1^n - \varepsilon_2 \nabla\Phi_2^n) = \frac{1}{j\omega}\left[\oint_{\partial F_n} (\nabla G_1 - \nabla G_2)\,(\mathbf{o}_n \cdot \hat{n}_c)\,dl' - \iint_{F_n} (\nabla G_1 - \nabla G_2)\nabla' \cdot (\mathbf{o}_n) ds'\right] \quad (54)$$

and, in an analogous manner, for the expansion of the magnetic scalar potential in (50), we can write

$$(\mu_1 \nabla\Psi_1^n - \mu_2 \nabla\Psi_2^n) = \frac{1}{j\omega}\left[\oint_{\partial F_n} (\nabla G_1 - \nabla G_2)\,(\mathbf{o}_n \cdot \hat{n}_c)\,dl' - \iint_{F_n} (\nabla G_1 - \nabla G_2)\nabla' \cdot (\mathbf{o}_n) ds'\right] \quad (55)$$

5. RESULTS

We compute the impedance elements in the resulting impedance matrices with great accuracy. We carry out the analytical extraction of the quasi-singular R^{-3} and R^{-1} contributions of the Kernels with traditional integrating schemes over triangles [1, 26, 27]. The remaining source contributions and the field testing integrals are computed numerically with a 9-point Gaussian quadrature rule. Interestingly, the Müller-formulation results in the advantageous cancelation of some R^{-3}-contributions. For example, the expression $(\nabla G_1 - \nabla G_2)$ in (54) and (55) shows a milder R^{-1}-dependence after the subtraction process [13]. Similarly, since $\mu_1 = \mu_2 = \mu_0$ in all tested cases, the subtraction $(\mu_1 \nabla G_1 - \mu_2 \nabla G_2)$ arising in (48) turns out also R^{-1}-dependent.

In our tests of RCS accuracy for the div-TO MoM-implementations we adopt sharp-edged objects with moderately small electrical dimensions (with electrical dimensions of wavelength fractions) for the following reasons: (i) the presence of sharp-edges is dominant in the scattering process and therefore their influence becomes relevant for any direction of observation; (ii) it is possible to assess the convergence of the computed RCS against the number of unknowns because the required computational requirements for very fine meshings stay within the available resources. In all the tested cases, we excite the bodies with a $+z$-propagating x-polarized plane wave. The adopted wavelength and free-space wavelength, respectively, for the perfectly conducting or dielectric bodies is 1 m.

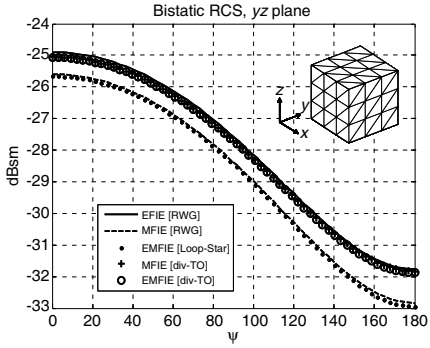

Figure 2. yz plane cut of the RCS computed with MFIE [div-TO], EMFIE [div-TO], EFIE [RWG], MFIE [RWG] and EMFIE [Loop-Star] for a PeC-cube with side 0.1 m meshed with 108 triangular facets and wavelength 1 m.

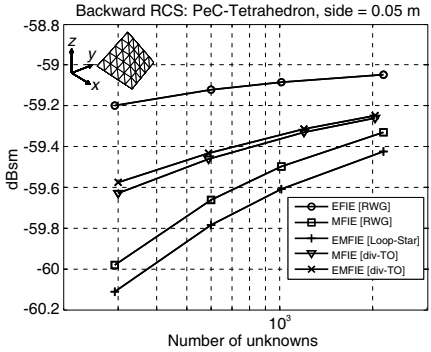

Figure 3. Backward RCS of a regular PeC-tetrahedron with side 0.05 m computed with MFIE [div-TO], EMFIE [div-TO], EFIE [RWG], MFIE [RWG] and EMFIE [Loop-Star]. The wavelength is 1 m.

In Figure 2, we present the computed RCS for a perfectly conducting cube with side 0.1 m discretized with 108 triangular facets. We see clearly how for this sharp-edged object the computed RCS patterns with the div-TO discretizations of the Second Kind Integral Equations, MFIE and EMFIE, MFIE [div-TO] and EMFIE [div-TO], respectively, reduce the observed discrepancy of the RWG and Loop-Star discretizations of the MFIE and the EMFIE, MFIE [RWG] and EMFIE [Loop-Star], with respect to the RWG discretization of the EFIE, EFIE [RWG].

In Figures 3 and 4, we show, respectively, the backward and forward RCS against the number of unknowns of the MoM-implementations EFIE [RWG], MFIE [RWG], MFIE [div-TO] and EMFIE [div-TO] for a perfectly conducting regular tetrahedron with side 0.05 m. The gain in RCS accuracy by adopting a div-TO discretization of MFIE and EMFIE under a given mesh is clearly better than increasing the number of unknowns for a RWG discretization by making the mesh finer. Also, we see that the improvement in the div-TO discretizations is in relative terms much better for less fine meshings, when the influence of the sharp-edges becomes more important. The same is observed in Figures 5 and 6 for a regular tetrahedron with bigger electrical dimensions, with side 1 m (one wavelength).

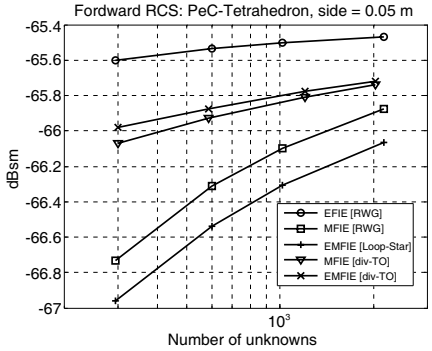

Figure 4. Forward RCS of a regular PeC-tetrahedron with side 0.05 m computed with MFIE [div-TO], EMFIE [div-TO], EFIE [RWG], MFIE [RWG] and EMFIE [Loop-Star]. The wavelength is 1 m.

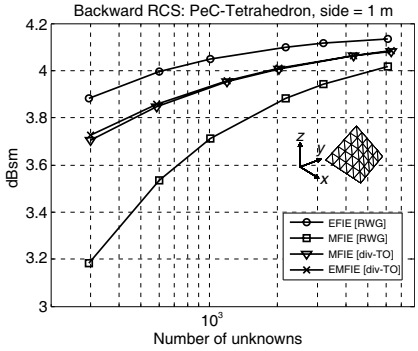

Figure 5. Backward RCS of a regular PeC-tetrahedron with side 1 m computed with MFIE [div-TO], EMFIE [div-TO], EFIE [RWG] and MFIE [RWG]. The wavelength is 1 m.

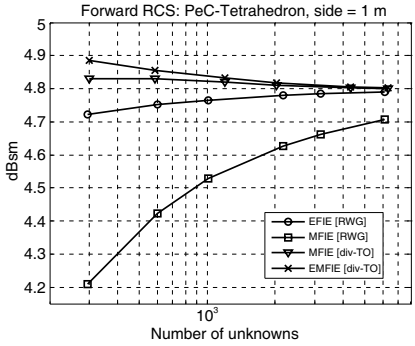

Figure 6. Forward RCS of a regular PeC-tetrahedron with side 1 m computed with MFIE [div-TO], EMFIE [div-TO], EFIE [RWG] and MFIE [RWG]. The wavelength is 1 m.

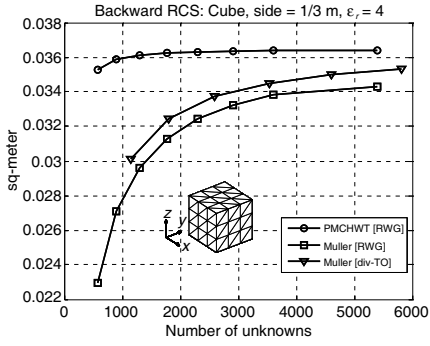

Figure 7. Backward RCS of a dielectric cube with $\varepsilon_r = 4$ with side 0.33 m computed with PMCHWT [RWG], Muller [RWG] and Muller [div-TO]. The free-space wavelength is 1 m.

In Figure 7, we validate our MoM-implementations for dielectrics through the backward RCS plot against the number of unknowns of a cube with side 0.33 m and relative permittivity of 4 (see Figure 3 of [14]). In Figures 8 and 9, we show the forward scattered RCS against the number of unknowns for two different sharp-edged moderately

small dielectric regular polyhedra, a cube and a tetrahedron, with low dielectric contrast (relative permittivities of 3 and 2) and side 0.1 m. Note how the observed RCS deviation now, in the dielectric case, for the RWG discretization of the Müller-formulation, Muller [RWG], is much lower, 0.3 dB at most for very coarse meshings, than in the perfectly conducting case for the RWG discretizations of the MFIE

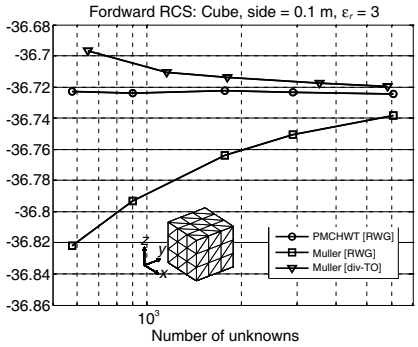

Figure 8. Forward RCS of a dielectric cube with $\varepsilon_r = 3$ and side 0.1 m computed with PMCHWT [RWG], Muller [RWG] and Muller [div-TO]. The free-space wavelength is 1 m.

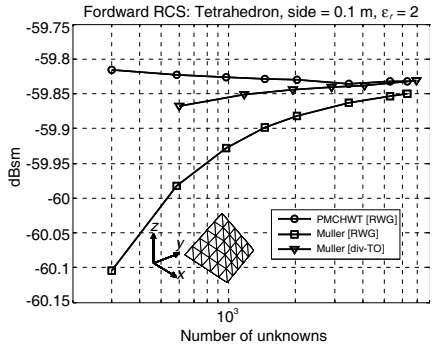

Figure 9. Forward RCS of a dielectric regular tetrahedron with $\varepsilon_r = 2$ and side 0.1 m computed with PMCHWT [RWG], Muller [RWG] and Muller [div-TO]. The free-space wavelength is 1 m.

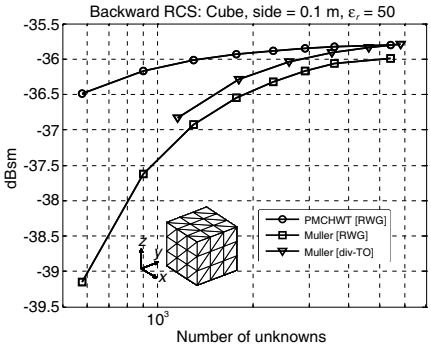

Figure 10. Backward RCS of a dielectric cube with $\varepsilon_r = 50$ and side 0.1 m computed with PMCHWT [RWG], Muller [RWG] and Muller [div-TO]. The free-space wavelength is 1 m.

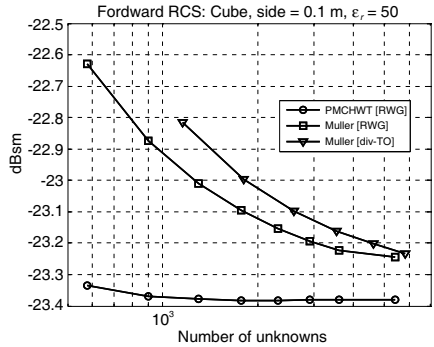

Figure 11. Forward RCS of a dielectric cube with $\varepsilon_r = 50$ and side 0.1 m computed with PMCHWT [RWG], Muller [RWG] and Muller [div-TO]. The free-space wavelength is 1 m.

or the EMFIE. For these two cases, the div-TO discretization of the Müller-formulation, Muller [div-TO], follows the RCS computed with the PMCHWT-formulation, PMCHWT [RWG], more closely than the RWG-discretization of the Müller-formulation, Muller [RWG].

In Figures 10 and 11, we show the backward and forward RCS against the number of unknowns for a cube with side 0.1 m and a high dielectric contrast ($\varepsilon_r = 50$). Now the observed RCS deviation for the discretizations of the Müller-formulation is bigger than for lower dielectric contrasts. In view of these figures, the RWG or the div-TO sets do not appear as competitive options with respect to the PMCHWT-formulation, which shows a more stable trend for convergence.

6. CONCLUSIONS

We present the Taylor-Orthogonal basis functions as a set of basis functions suitable for the discretization in Method of Moments of two types of Second Kind Integral Equations: (i) the recently introduced Electric-Magnetic Field Integral Equation (EMFIE), for conductors, and (ii) the Müller formulation, for homogeneous or piecewise homogeneous dielectrics. These basis functions are derived from the 2D-linear Taylor's expansion of the current around the geometric centers of the facets arising from the discretization. We define the divergence-Taylor-Orthogonal [div-TO] and the curl-Taylor-Orthogonal [curl-TO] sets as the basis functions capturing, respectively, the divergence of the current and the normal component of the curl of the current at the centroids of triangles. We show that the div-TO implementation of the EMFIE reduces the observed RCS discrepancy of the RWG and Loop-Star discretizations of the MFIE and EMFIE, respectively, for moderately small sharp-edged conductors. Moreover, in view of our tests with moderately small sharp-edged dielectrics, we observe that the div-TO discretization of the Müller-formulation better approaches the RCS computed with the PMCHWT-formulation for sharp-edged objects with low contrasts. For a cube with high-dielectric contrast, both RWG and div-TO discretizations of the Müller-formulation show a bigger deviation with respect to PMCHWT, which shows a stable trend of convergence in any case. The facet-oriented discretization of the Müller-formulation presented in this paper allows a straightforward implementation of the Müller-formulation for composite piecewise homogeneous dielectric objects. Indeed, assigning unknowns to facets avoids imposing the normal continuity of the expanded current across the junctions arising from the intersection of several dielectric regions, as it is required when the edge-oriented RWG basis functions are adopted [28].

ACKNOWLEDGMENT

This work was supported by the Spanish Interministerial Commission on Science and Technology (CICYT) under Projects TEC2010-20841-C04-02, TEC2007-66698-C04-01/TCM, TEC2009-13897-C03-01 and CONSOLIDER CSD2008-00068.

REFERENCES

1. Hodges, R. E. and Y. Rahmat-Samii, "The evaluation of MFIE integrals with the use of vector triangle basis functions," *Microwave and Optical Technology Letters*, Vol. 14, No. 1, 9–14, Jan. 1997.
2. Graglia, R. D., D. R. Wilton, and A. F. Peterson, "Higher order interpolatory vector bases for computational electromagnetics," *IEEE Transactions on Antennas and Propagation*, Vol. 45, No. 3, 329–342, Mar. 1997.
3. Rius, J. M., E. Ubeda, and J. Parrón, "On the testing of the magnetic field integral equation with RWG basis functions in method of moments," *IEEE Transactions on Antennas and Propagation*, Vol. 49, No. 11, 1550–1553, Nov. 2001.
4. Rao, S. M., D. R. Wilton, and A. W. Glisson, "Electromagnetic scattering by surfaces of arbitrary shape," *IEEE Transactions on Antennas and Propagation*, Vol. 30, No. 3, 409–418, May 1982.
5. Wilton, D. R. and J. E. Wheeler, III, "Comparison of convergence rates of the conjugate gradient method applied to various integral equation formulations," *Progress In Electromagnetics Research*, Vol. 5, 131–158, 1991.
6. Ubeda, E. and J. M. Rius, "MFIE MoM-formulation with curl-conforming basis functions and accurate Kernel-integration in the analysis of perfectly conducting sharp-edged objects," *Microwave and Optical Technology Letters*, Vol. 44, No. 4, Feb. 2005.
7. Ergül, Ö. and L. Gürel, "The use of curl-conforming basis functions for the magnetic-field integral equation," *IEEE Transactions on Antennas and Propagation*, Vol. 54, No. 7, 1917–1926, Jul. 2006.
8. Ubeda, E. and J. M. Rius, "Comments on "The use of curl-conforming basis functions for the magnetic-field integral equation"," *IEEE Transactions on Antennas and Propagation*, Vol. 56, No. 7, 2142, Jul. 2008.
9. Ergül, Ö. and L. Gürel, "Improving the accuracy of the magnetic

field integral equation with the linear-linear basis functions," *Radio Science*, Vol. 41, 2006, RS4004, doi:10.1029/2005RS003307.

10. Ubeda, E. and J. M. Rius, "Novel monopolar MoM-MFIE discretization for the scattering analysis of small objects," *IEEE Transactions on Antennas and Propagation*, Vol. 54, No. 1, 50–57, Jan. 2006.
11. Müller, C., *Foundations of the Mathematical Theory of Electromagnetic Waves*, Springer, Berlin, Germany, 1969.
12. Chao, J. C., Y. J. Liu, F. J. Rizzo, P. A. Martin, and L. Udpa, "Regularized integral equations and curvilinear boundary elements for electromagnetic wave scattering in three dimensions," *IEEE Transactions on Antennas and Propagation*, Vol. 43, No. 12, 1416–1422, Dec. 1995.
13. Ylä-Oijala, P. and M. Taskinen, "Well-conditioned Müller formulation for electromagnetic scattering by dielectric objects," *IEEE Transactions on Antennas and Propagation*, Vol. 43, No. 12, Dec. 1995.
14. Ylä-Oijala, P., M. Taskinen, and S. Järvenpää, "Surface integral equation formulations for solving electromagnetic scattering problems with iterative methods," *Radio Science*, Vol. 40, No. 6, Nov. 2005, RS6002.
15. Poggio, A. J. and E. K. Miller, "Integral equation solutions of threedimensional scattering problems," *Computer Techniques for Electromagnetics*, Vol. 4, R. Mittra, Ed., Pergamon Press, Oxford, U.K., 1973.
16. Wu, T. K. and L. L. Tsai, "Scattering from arbitrarily-shaped lossy dielectric bodies of revolution," *Radio Science*, Vol. 12, 709–718, Sep.–Oct. 1977.
17. Chang, Y. and R. F. Harrington, "A surface formulation for characteristic modes of material bodies," *IEEE Transactions on Antennas and Propagation*, Vol. 25, 789–795, Nov. 1977.
18. Ubeda, E., J. M. Tamayo, and J. M. Rius, "Orthogonal basis functions for the discretization of the magnetic-field integral equation in the low frequency regime," *European Conference on Antennas and Propagation (EUCAP)*, Barcelona, Apr. 12–16, 2010.
19. Ubeda, E. and J. M. Rius, "New electric-magnetic field integral equation for the scattering analysis of perfectly conducting sharp-edged objects at very low or extremely low frequencies," *IEEE International Symposium on Antennas and Propagation*, Toronto, Jul. 11–17, 2010.

20. Wu, W., A. W. Glisson, amd D. Kajfez, "A study of two numerical procedures for the electric field integral equation at low frequency," *Appl. Computat. Electromagn. Soc. J.*, Vol. 10, No. 3, Nov. 1995.
21. Lee, J., R. Lee, and R. J. Burkholder, "Loop star basis functions and a robust preconditioner for EFIE scattering problems," *IEEE Transactions on Antennas and Propagation*, Vol. 51, No. 8, Aug. 2003.
22. Trintinalia, L. C. and H. Ling, "First order triangular patch basis functions for electromagnetic scattering analysis," *Journal of Electromagnetic Waves and Applications*, Vol. 15, No. 11, 1521–1537, 2001.
23. Van Bladel, J., *Singular Electromagnetic Fields and Sources*, Clarendon Press, Oxford, 1991.
24. Ubeda, E. and J. M. Rius, "Monopolar divergence-conforming and curl-conforming low-order basis functions for the electromagnetic scattering analysis," *Microwave and Optical Technology Letters*, Vol. 46, No. 3, 237–241, Aug. 2005.
25. Taskinen, M., "Electromagnetic surface integral equations and fully orthogonal higher order basis functions," *IEEE International Symposium on Antennas and Propagation*, San Diego, Jul. 5–12, 2008.
26. Graglia, R. D., "On the numerical integration of the linear shape functions times the 3D's Green's function or its gradient on a plane triangle," *IEEE Transactions on Antennas and Propagation*, Vol. 41, No. 10, 1448–1455, Oct. 1993.
27. Wilton, D. R., S. M. Rao, A. W. Glisson, D. H. Schaubert, O. M. Al-Bundak, and C. M. Butler, "Potential integrals for uniform and linear source distributions on polygonal and polyhedral domains," *IEEE Transactions on Antennas and Propagation*, Vol. 32, No. 3, 276–281, Mar. 1984.
28. Ylä-Oijala, P., M. Taskinen, and J. Sarvas, "Surface integral equation method for general composite metallic and dielectric structures with junctions," *Progress In Electromagnetics Research*, Vol. 52, 81–108, 2005.